Large-scale Modeling and Demand Response Control of Electric Water Heaters with Energy Star and CTA-2045 Control Types in Distribution Power System

Huangjie Gong, *Student Member, IEEE*, Evan S. Jones, *Student Member, IEEE*, A H M Jakaria, Aminul Huque, *Member, IEEE*, Ajit Renjit, *Member, IEEE* and Dan M. Ionel, *Fellow, IEEE*

Abstract: The paper proposes a generalized energy storage (GES) model for battery energy storage systems (BESS), electric water heaters (EWH) and heating, ventilation, and air-conditioning (HVAC) systems to enable demand response control complying to Energy Star and CTA-2045 standards. The demand response control has been implemented in the DER integration testbed, which was originally developed by EPRI, to demonstrate that the "energy content" and "energy take" for BESS and EWH with mixing valve technology are comparable for typical residential ratings. A distribution power system was modeled using the modified IEEE 123-bus feeder system, measured residential loads, and EWH power simulated based on realistic hot water draws. The demand response control, which complies to CTA-2045 standards was implemented to the EWH considering the energy take values. Results including the water temperature and energy take for each EWH, as well as the total power and voltages for all the bus of the IEEE-123 bus feeder were analyzed.

***Index Terms*—Battery Energy Storage System (BESS), Electric Water Heater (EWH), Energy Storage, ANSI/CTA-2045-B, Energy Star, Energy Take, Home Energy Management (HEM), Demand Response (DR), Aggregation, Distribution Power System, OpenDSS, Voltage Variation.**

I. Introduction

The advancement of smart home and grid technologies and the associated electric power system integration studies relies on individual and combined simulators for buildings, such as EnergyPlus, and circuit networks, e.g., OpenDSS, MATPOWER, GridLAB-D, etc. [1]. The Distributed Energy Resources (DER) integration testbed, which includes open-source simulation software, was originally developed by the Electric Power Research Institute (EPRI), comprises multiple layers for controls, devices, and circuits, and is able to communicate using protocols that are typically employed for hardware components [2], [3]. Using this technique, the DER integration testbed can be used with a combination of real physical devices and/or with their equivalent model-in-the-loop (MIL) software implementation. The advantages of the MIL approach include cost-effective development and testing in a realistic set-up and the ability to largely scale-up studies with minimal hardware [4], [5].

Energy storage devices and systems, which can be electric, such as battery energy storage systems (BESS), or thermal, such as electric water heaters (EWH) or heating, ventilation and air conditioning (HVAC) systems [6], are essential in order to ensure an optimal energy management and power flow within the modern grid with DER. This method of hybrid energy storage can reduce required BESS capacity by up to 30% while providing the same capability [7]. To support technology development and standard-type implementation that would enable wide scale industrial and utility deployment, Energy Star, a program conducted by the Environmental Protection Agency (EPA) and Department of Energy (DOE), provides general specifications for energy parameters and demand response (DR) functionalities [8].

For EWH, these specifications are typically implemented using the Consumer Technology Association (CTA) 2045 standard [9], and success has been reported at the individual residential and utility aggregated levels [10], [11]. In principle, the combined Energy Star and CTA-2045 specifications and concepts such as "energy capacity", "energy content", and "energy take" and DER commands, such as "load up", "shed", etc., can be extended to any energy storage device and system, enabling a unified approach at the system level.

Modeling of EWH energy use at the individual level to be employed in a DER testbed may be performed through physics-based equations to model the thermal losses to the environment and water consumption as well as for the contribution from the heating element [12]. In addition to these mathematical representations, estimation through measured data was utilized to determine certain parameters of the physical model. Typical DHW schedules, such as those provided by the CBECC-Res Compliance Software Project [13], are very useful resources for performing realistic community-level simulation studies.

The IEEE test bus systems are available in OpenDSS for the studies of large scale DER implementation and DR control [14], [15]. These distribution system models in combination with proper control strategies and by considering the behavior of EWHs in an aggregated manner enables the community-

H. Gong, E. S. Jones, and D. M. Ionel are with the SPARK Laboratory, Department of Electrical and Computer Engineering, University of Kentucky, Lexington, KY, USA (e-mail: huangjie.gong@uky.edu, sevanjones@uky.edu, dan.ionel@ieee.org).

A H M Jakaria, Aminul Huque, and Ajit Renjit are with Tennessee Valley Authority, USA (e-mails: ajakaria@epri.com, mhuque@epri.com, arenjit@epri.com).

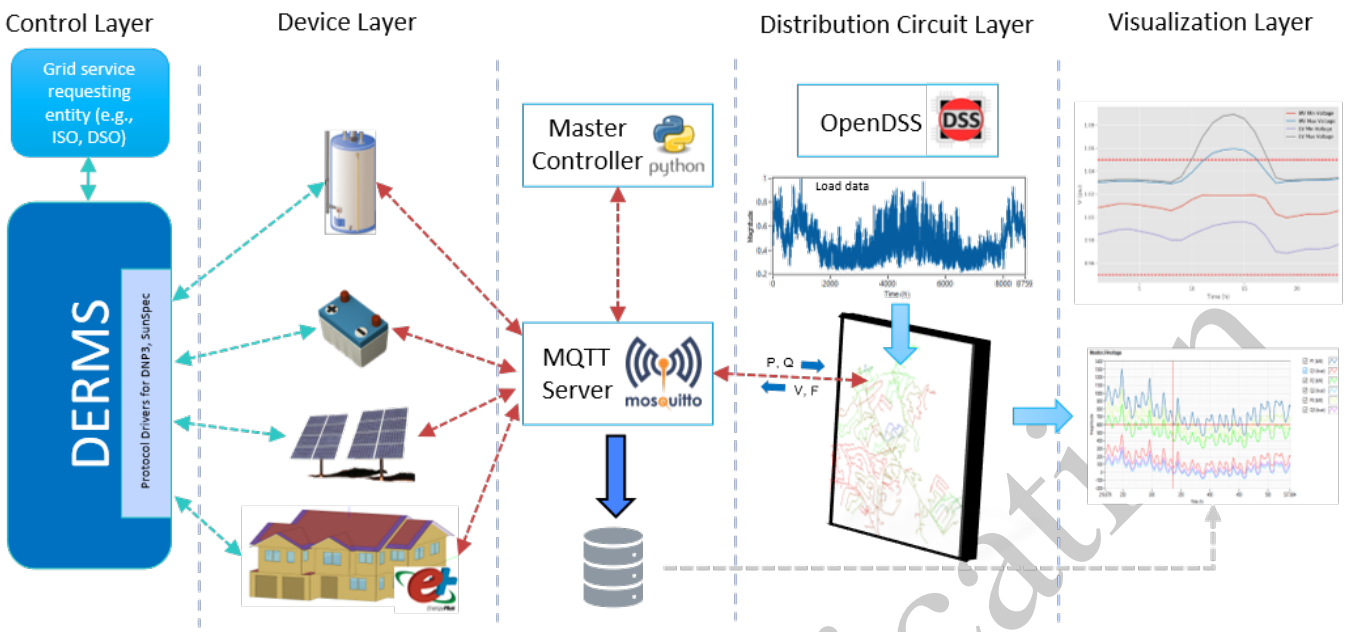

Figure 1. The architecture of EPRI's DER integration testbed. Models-in-the-loop (MIL) are employed at the device layer. The paper proposes unified models for the battery energy storage systems (BESS) and electric water heaters (EWH) suitable for Energy Star and CTA-2045 control types, which are issued by a distributed energy resource management system (DERMS). The MILs are to communicate with the distribution system simulator, which is OpenDSS for this study, through the Message Queuing Telemetry Transport (MQTT), which enables distribution-level simulation of control schemes.

level study of EWHs as controllable residential BESSs. When deployed as an aggregate entity, EWHs can be considered assets for grid services [16]. It has been shown that EWHs at aggregated level can provide equivalent grid service as batteries [17].

A research gap remains for large scale simulation of EWHs in a distribution power system. A study to help with this gap in literature should fulfill three important criteria. First, each EWH should have its own hot water draw, which should be realistic and representative of typical usage. Second, the impact of DR control on EWHs should also consider both power demand and the voltages of buses at which the associated residences are connected. Also, the change of total load in the power system should consider the power losses. Third, the DR control signals for EWHs should comply with the CTA-2045 standards.

This paper is a substantially expanded follow up of a previous conference paper by the same research group, which introduced the EPRI's DER testbed and defined the GES concept including EWH and BESS [18]. In addition to the previous conference paper, EWHs were simulated on a large scale each with their own daily hot water draw. The modified IEEE 123-bus feeder system was simulated with residences comprising of measured load data and simulated EWH power. The DR control complying to CTA-2045 standard was tested and discussed.

The main contributions include: (1) verification of EWHs as equivalent energy storage; (2) a proposed method for batch modeling of individual EWHs based on realistic hot water flow; (3) combined dynamic simulation of individual EWHs and a distribution power sustem with realistic residential loads; (4) application of CTA-2045 standard-based DR on EWH at a large scale; (5) the analysis of EWH DR impact on an example distribution power system, including voltage variation.

Following the introduction, the EPRI DER testbed is introduced, and the GES concept is then defined in Section II. Case studies that apply the EWH as energy storage are presented in Section III. The modeling for multiple EWHs with realistic DHW draw is provided in Section IV and V. Results for the co-simulation of EWHs and the distribution power system are presented and discussed in Sections VI. The final section includes the conclusions of this work.

II. EPRI's DER Integration Testbed and Definitions of Generalized Energy Storage

The EPRI's DER integration testbed (Fig. 1) simulates power system models with real world communication systems and DER models. The testbed can assess the control functionality and communication interoperability of the Distributed Energy Resources Management System (DERMS) and can evaluate different control strategies for any circuit. It also supports real world communication systems by incorporating industry standard protocols, such as the CTA-2045 standard, Energy Star specifications, DNP3, and SunSpec Modbus.

The DER integration testbed has four layers in its architecture: control, device, circuit, and visualization and analytics (Fig. 1). The circuit layer contains a power system simulator, such as OpenDSS or Cyme, to model the feeder and calculate powerflow. The visualization and analytics layer provides the user with actionable information to analyze the full system.

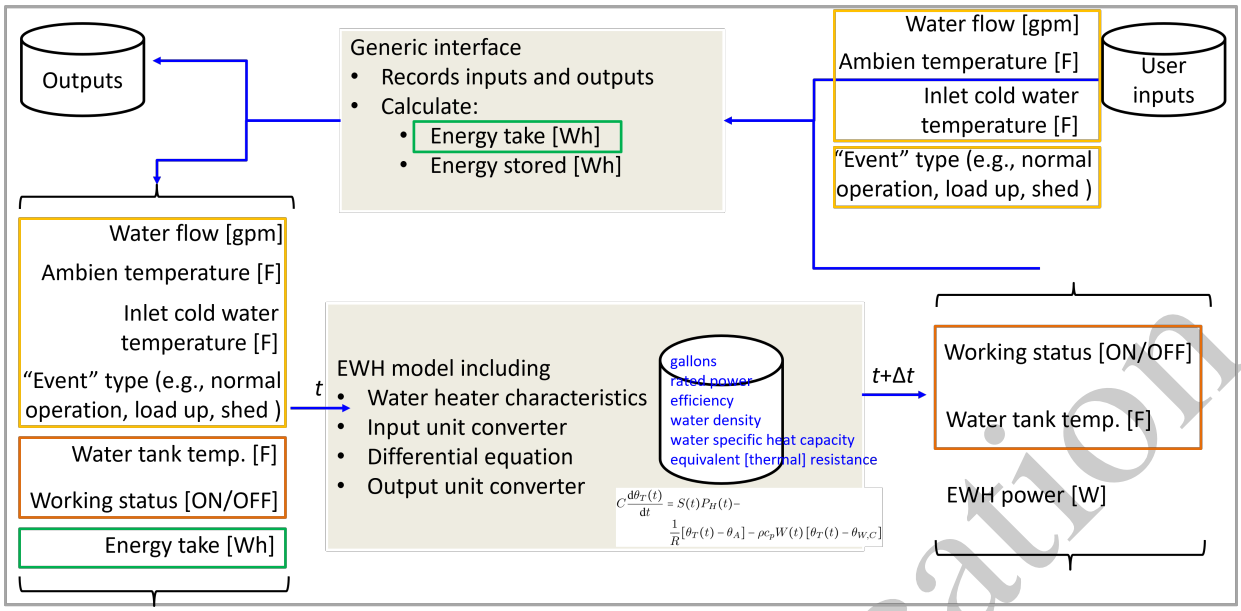

Figure 2. Schematic of the Model-In-the-Loop (MIL) for an Electric Water Heater (EWH). The computer code is implemented in C# under Visual Studio 2020 and communications with the EPRI's DER integration testbed follow the CTA-2045 standard for Energy Star commands.

The control layer manages DER in the device layer using control strategies that may be user-built or commercial.

OpenDERMS is an EPRI developed reference control tool that can aggregate, optimize and manage large number of DER to provide grid services while enabling customer benefits. The devices in the device layer are implemented as software simulators that emulate real world DER characteristics and incorporate built-in commercial communication interfaces for common industry protocols. The device and circuit layers communicates through the Message Queuing Telemetry Transport (MQTT) protocol, which is an effective communication tool for IoT devices and has great potential for facilitating co-simulation of multiple DER ecosystems [19]. Utilizing this tool enables distribution-level simulation of demand response (DR) control schemes and co-simulation of the distribution system simulator, model-in-the-loop (MIL), and other device-level simulators such as EnergyPlus, a whole building energy simulation program.

The EPRI's DER integration testbed for energy storage systems is of particular interest for this study as it was utilized for the simulation of an EWH that is treated as an energy storage system [3]. The simulator is capable of various smart functions, such as connection/disconnection, charging/discharging, volt-VAR curve input, and generation level and power factor adjusting. The EWH MIL was simulated in the paper and connected to EPRI's DER integration testbed (Fig. 2).

The Generalized Energy Storage (GES) in a residence includes BESS, EWH, and the HVAC system. For a BESS, the "current available energy storage capacity" is calculated as follows:

$$E_{C,B}(t) = \overline{E_{B,R}} \cdot (SOC_{B,max} - SOC_B(t)), \quad (1)$$

where $\overline{E_{B,R}}$ is the rated energy capacity of the BESS; $SOC_{B,max}$, the maximum allowed SOC.

Most CA-2045 available EWHs only provide the "energy take" instead of the water temperature inside the tank, which is hard to measure as it is stratified. In this paper, the "energy content of the stored water" for the EWH is defined as:

$$E_W(t) = V\rho c_p \theta_T(t), \quad (2)$$

where V is water tank volume; ρ, density of water; c_p, specific heat capacity of water; θ_T, the average temperature in the water tank. Based on (2), the "current available energy storage capacity" for a water heater is calculated by referring to the set point, as follows:

$$E_{C,W}(t) = \overline{E_{W,S}} - E_W(t), \quad (3)$$

where $\overline{E_{W,S}} = V\rho c_p \theta_{T,S}$ is the maximum energy capacity for the EWH, defined by $\theta_{T,S}$, the set point. The "energy take" is defined as follows:

$$E_{T,W}(t_2 - t_1) = E_W(t_2) - E_W(t_1). \quad (4)$$

The HVAC system is regarded as an energy storage and its equivalent SOC is defined as:

$$SOC_H(t) = \frac{\theta_{max} - \theta_I(t)}{\theta_{max} - \theta_{min}}, \quad (5)$$

where the θ_{max} and θ_{min} are the maximum and minimum room temperature, respectively; θ_I, the indoor temperature. The energy storage capacity of the HVAC system, $\overline{E_{H,C}}$, is defined as the input electricity needed to change the room temperature from the maximum to the minimum with a fixed outside temperature [20]. The "current available energy storage

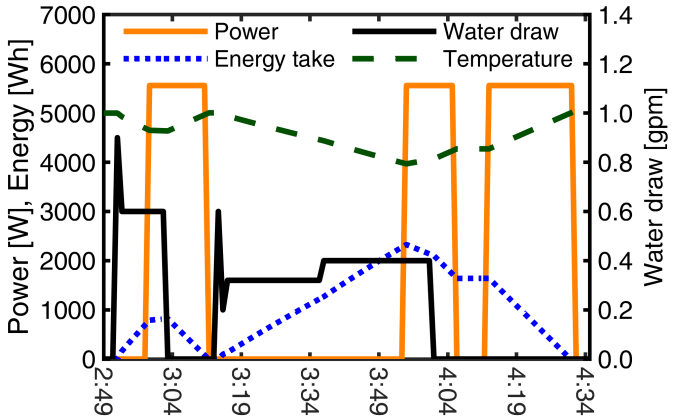

Figure 3. Example of simulated EWH "Shed Event" corresponding to the experimental data illustrated in Fig. 4. Based on DR control signals, the "energy take" capacity was increased from 900Wh to 2,200Wh, resulting in a shift/delay of the water heating process.

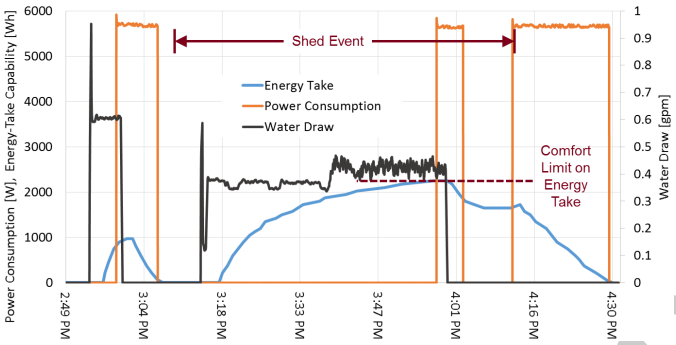

Figure 4. Experimental data, previously reported by NREL/EPRI [10], and employed for the satisfactory validation of the proposed EWH MIL. The "Shed Event" occurs from 3:10 to around 4:10, which causes the "energy take" range to increase and the heating process to be postponed while maintaining occupant comfort.

capacity" for the HVAC system calculated as:

$$E_{C,H}(t) = \overline{E_{H,C}} \cdot (1 - SOC_H(t)). \quad (6)$$

III. Case Study for EWH as Energy Storage

Two cases, which were based on experimental results, were studied to validate the EWH as a MIL in the EPRI's DER integration testbed. In the first case, the simulation results of a resistive EWH was validated against the experimental data from an EPRI performance test on a CTA-2045 compatible EWH [10]. The "energy take" values for all the DR events were based on the case study published in [10]. The tank temperature and the "energy take" values were calculated as the EWH responded to the "Shed event" signal (Fig. 3). The temperature and water draw are referred in p.u., where the base values for temperature and hot water flow are 140 F and 1 gallon per minute (GPM), respectively. The comparison between Figs. 3 and 4 shows satisfactory accuracy of the simulated EWH model with CTA-2045 availability.

The second case was based on the experiment from the

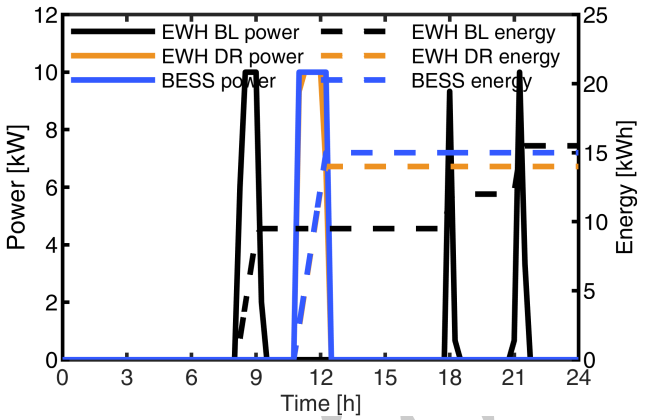

Figure 5. Comparative study of energy storage with BESS and EWH, including typical/normal base line (BL) and demand response (DR) schedules. For BL operation, the EWH has a morning and two evening peak power cycles. The BESS schedule was adjusted to allow comparison with a EWH study for DR load shifting around noon, which may align well with PV generation, if available.

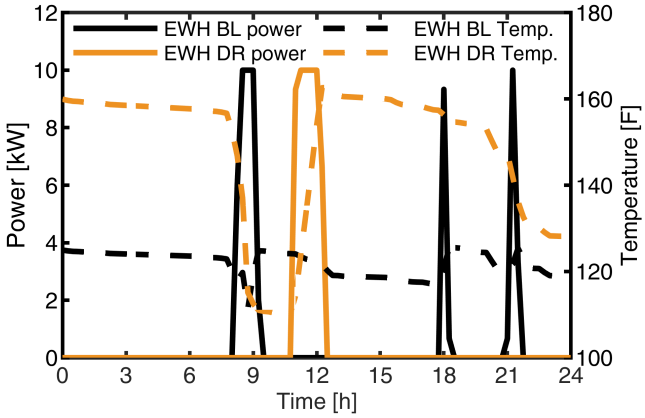

Figure 6. Power draw and water tank temperature for an EWH operating under BL and DR studied schedules. The high water temperature in the tank may be enabled by special mixing valve technologies.

EPRI SHINES demonstration, which was launched in 2016 by the DOE to develop and demonstrate technologies that enable sustainable and holistic integration of energy storage with solar PV [21]. In this paper, the EWH loads of the two houses, as well as the BESS, solar PV, pool pump and HVAC were tested in the field. The different EWH loads and BESS charging schedule as well as the corresponding energy and aggregated power of the two EWHs are provided for a comparative study (Fig. 5).

The example charging schedule for the BESS resulted in a similar power rating when compared to the EWH DR power (Fig. 6). Mixing valve technology was used to guarantee occupant safety when the temperature in the water tank was high. The EWH under DR can be programmed at night to boost the tank temperature to the same value as the beginning of the day.

The EPRI SHINES demonstration provides timely data with a resolution of 15 minutes for the power flow at the transformer

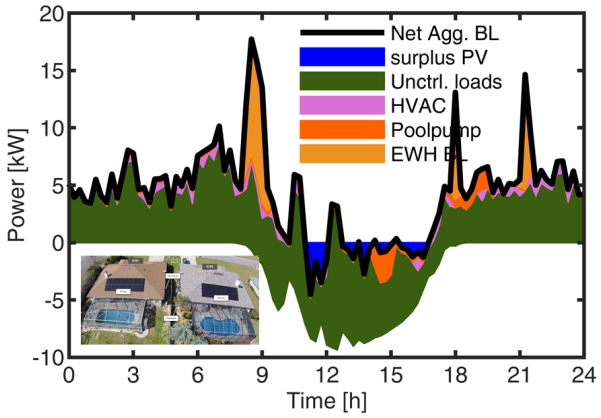

Figure 7. Combined experimental and simulated power flow on an example February day for two smart homes, which are located in Florida and were developed as part of the EPRI SHINES DOE project (photo inset). The EWH simulations were performed with the proposed MIL.

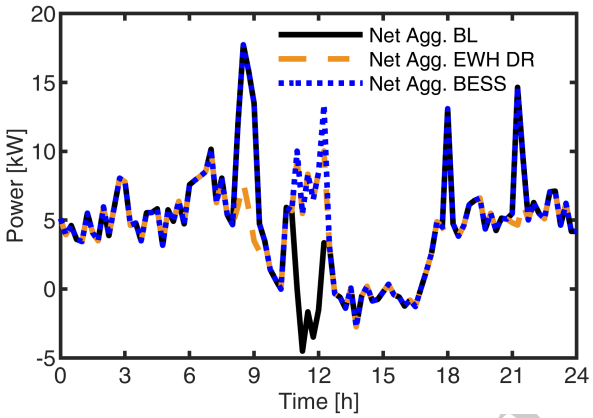

Figure 8. Case studies for the aggregated net power flow at the distribution level. For the proposed control, during the day, a substantial portion of the solar PV generated energy was locally stored in the EWH or BESS.

where four houses were connected. Two of the four houses have their own solar PV installations, HVACs, pool pumps, and other non-DER loads monitored by the SHINES project. The non-DER loads of the monitored houses were added to the total power of the other two houses, and were labeled as "uncontrollable loads" at the distribution level (Fig. 7).

The EWH provided the energy storage capacity for the surplus PV generation as the BESS (Fig. 5). The net flow at the aggregated level was reduced due to the DR control, as shown in Fig. 8. Shifting the EWH load also reduced the peaks in the afternoon and evening.

IV. The Realistic Hot Water Draw and EWH Model with CTA-2045 Control

Hot water draw from the CBECC-Res data set was named as "XDY". X is the number of bedrooms and X∈{1,2,3,4,5}. CBECC-Res water heater draw has three types of days: weekdays (D), weekends (E), and holidays (H). Only type "D" was considered in this study. Y is the Y^{th} profiles for one category and Y∈{0,1,2,3,4,5,6,7,8,9}. The value for Y is only the natural sequence for different profiles and does not attribute to any specific day. For example, '3D8' is the 9^{th} weekday profile for a 3 bedroom house, and it represents a user behavior which could occur at any weekday.

Table I
Percentage and Number of Houses with Different Bedroom Numbers

Bedrooms	Percentage (%)	Number
0 & 1	2.1 + 8.2	36
2	25.8	91
3	42.8	151
4	16.7	59
5+	4.5	16

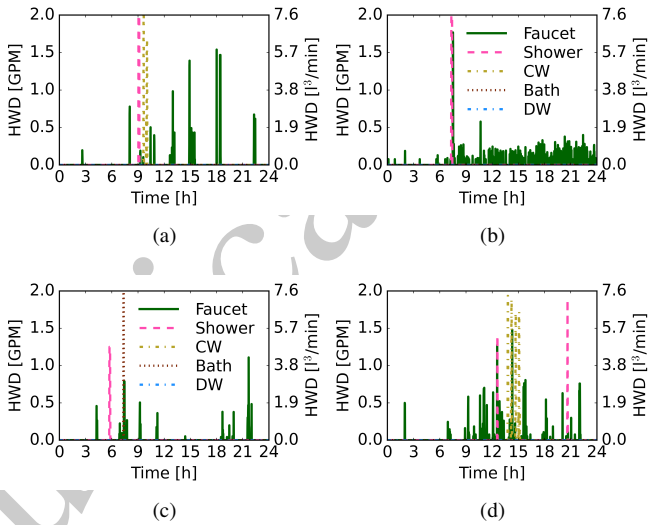

Figure 9. Example hot water draws from CBECC-Res data. Shown are four examples for (a) 1D7; (b) 2D6; (c) 3D3; (d) 4D3.

In this study, there were 36 residences with 1 bedroom (Table I), based on the survey published by the United States Census Bureau [22]. Therefore, 36 hot water draw were selected randomly as "1DY" (Y∈{0,1,2,3,4,5,6,7,8,9}) with repetition, i.e., some profiles were selected more than once. Similar procedures were performed for the other residences with more than 1 bedroom, and a total of 353 hot water draw profiles were selected based on the 50 representative hot water profiles from CBECC-Res.

The daily hot water draw profiles in CBECC-Res include the hot water draw (HWD) at different fixtures: faucet, shower, cloth washer (CW), bath, and dishwasher (DW) (Fig. 9). The temperature for hot water and cold water, and the hot water fraction of end use were concluded in [23]. The end use temperature for the fixtures were calculated (Table II).

The hot water flow at the outlet of the water tank was calculated using the water flow balance and energy balance, as follows:

Table II
HOT WATER FRACTION AND END USE TEMPERATURE OF FIXTURES.

End use	Hot water fraction	End use Temp. [F]
Faucet	0.50	95
Shower	0.66	105
Clothwasher	0.22	78
Bath	0.66	105
Dishwasher	1.00	125

$$\dot{V}_H + \dot{V}_C = \sum \dot{V}_i, \tag{7}$$

$$\dot{V}_H \theta_T(t) + \dot{V}_C \theta_{W,C} = \sum \dot{V}_i \theta_i, \tag{8}$$

where $\dot{V}_H$ is the water flow at the outlet of water tank; $\dot{V}_C$, water flow of cold water; $\dot{V}_i$, water flow at fixture; $\theta_T(t)$, the water temperature in the tank; $\theta_{W,C}$, cold water temperature; θ_i, end use temperature listed in Table II.

The 1R1C gray-box model of EWH is used for the calculation of water temperature with three major effects, i.e., the input electric power, the standby heat loss, and the hot water draw activities, as:

$$C\frac{\mathrm{d}\theta_T(t)}{\mathrm{d}t} = S(t)P_H(t) - \frac{1}{R}[\theta_T(t) - \theta_A] - \rho c_p W(t)\,[\theta_T(t) - \theta_{W,C}]\,. \tag{9}$$

C and $S(t)$ are the equivalent thermal capacitance and On/Off status, defined respectively, as:

$$C = V \cdot \rho \cdot c_p. \tag{10}$$

$$S(t) = \begin{cases} 0, & \text{if } S(t-1) = 1 \;\&\; E_{T,W}(t) \le Q_{T,min}(t) \\ 1, & \text{if } S(t-1) = 0 \;\&\; E_{T,W}(t) \ge Q_{T,max}(t) \\ S(t-1), & \text{otherwise,} \end{cases} \tag{11}$$

where $Q_{T,min}$ and $Q_{T,max}$ are the energy take levels, which differ for demand response events (Table III) [10] Other parameters are the same as the Table 3 from [24]. The energy take at a given time point $E_{T,W}(t)$ was referred to the starting point of the simulation and (4) is rewritten as:

$$E_{T,W}(t) = E_W(t) - E_W(0). \tag{12}$$

For the Normal operation event, increased hot water flow causes the energy take level to be lower. For the shed event, the energy take levels are much higher to allow for more hot water draw while keep the EWHs Off. The EWH would be On during the shed event when the energy take is too high to guarantee the user comfort. For the load up event, the EWH would be On even if the energy take is low.

Table III
WATER HEATER CONDITION AS CHARACTERIZED BY ENERGY TAKE LEVELS

Event	Energy take levels (Q_T) [Wh]	
	Minimum	Maximum
Normal operation	0	300: ≥ 1 GPM 600: ≥ 0.3 GPM 900
Shed	1800	2250
Load up	0	300

Table IV
EVENT TYPE AND DURATION

Event	Duration
Shed	[7:00,10:00) ∪ [17:00,19:00)
Load up	[6:00,7:00) ∪ [11:00,16:00)
Normal operation	Other time

V. CASE STUDY FOR AGGREGATED EWH MODELING

A total of 353 houses were connected to the IEEE 123-bus feeder and the numbers for different house type is presented in Table I, as explained in the previous section. Demand response control listed in Table IV was applied to all the EWHs in the same distribution system. This represents the worst scenario for the simulated subdivision, but even so, as presented in the following section, the voltages violation in the power system was still within the tolerance of 5%. For utilities serving large areas, the simulated distribution system is one subdivision of the larger system, and the simulated EWHs in this subdivision could be controlled as one batch. Therefore, the peak power for EWHs do not happen at the same time for the upper system. Within the subdivision, a sequential control method spreading out the turning On operation of EWHs, might be used to reduce the peak caused by rebound effect [6].

The initial water temperature in the tanks for all simulated EWHs were evenly distributed between 115F and 135F, noted as $\mathcal{U}(115F, 135F)$. The initial energy take for all simulated EWHs were evenly distributed between 0 and 1000Wh, noted as $\mathcal{U}(0, 1000Wh)$. The simulation results of On/Off status for all 353 EWHs demonstrate the antedated and postponed peak under CTA-2045 control (Fig. 10). The shadowing parts for the controlled case (bottom) indicate the duration when the DR control signals were implemented.

The peaks caused by load up event and the rebound effect are presented in the aggregated power for all the simulated EWHs (Fig. 11). The rebound effect at 9:00 during the shed event was caused by temperature recovering to maintain user comfort. It is observed by comparing the two shed events that the longer the event, the larger the rebound peak afterwards.

For the case without DR (Fig. 12, top), most of the EWHs had the energy take value between [0,1000Wh]. The outliers, which are represented by red dots, were caused by high hot water draw. Most of the outliers appeared in the morning and reflected the high water usage for residences at that time.

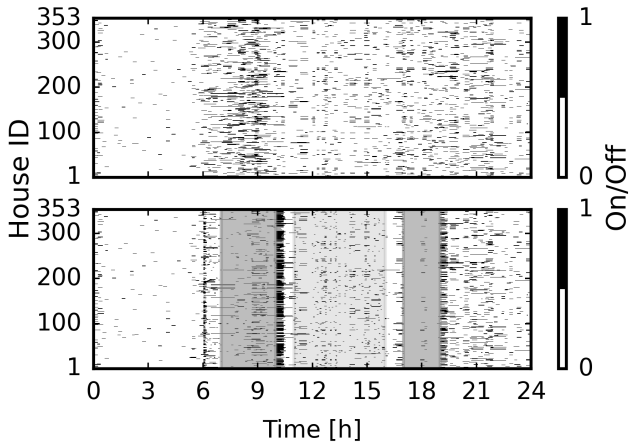

Figure 10. NEW FIGURE–Working status of the EWH without control (top) and with CTA-2045 control (bottom). The shed command in the morning and evening postpone most of the EWHs to be On.

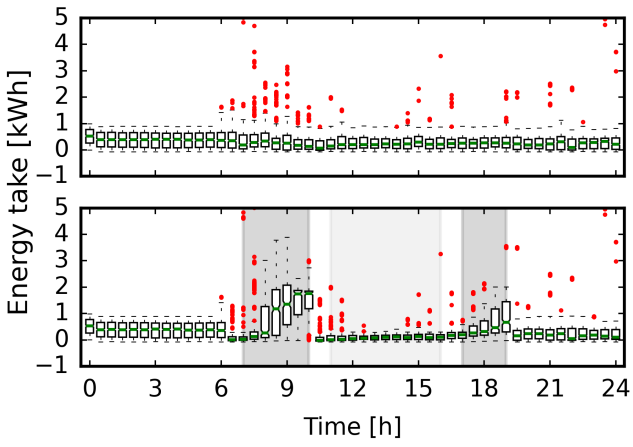

Figure 12. NEW FIGUREE–Energy take of the EWHs without control (top) and with CTA-2045 control (bottom). The shed command allowed more energy take while the load up did less.

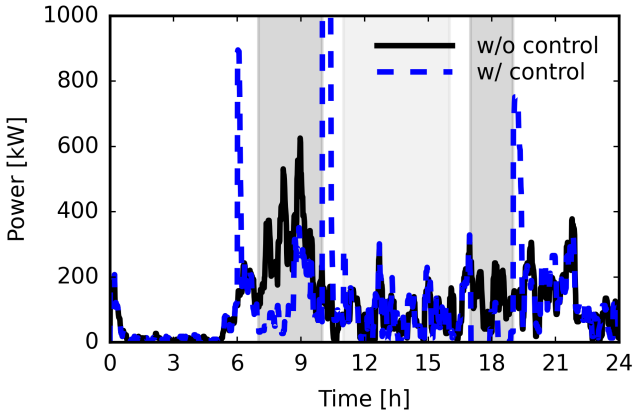

Figure 11. NEW FIGURE–Aggregated power for all the simulated EWHs. The shed command postponed the heating power and reduced the peak power during the DR control period in the morning and evening, but also caused the rebound afterwards.

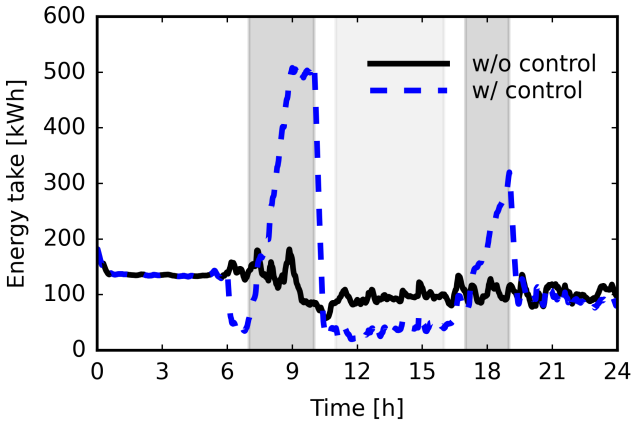

Figure 13. NEW FIGURE–Aggregated energy take for all the simulated EWHs. The shed command in the morning and evening resulted in high energy take. When the load up command was implemented in the afternoon, energy take was kept at a low level.

The minimum energy take values for shed events stayed at 0 instead of 1,800Wh as stated in Table III because some EWHs did not have hot water draw. Therefore, even when the minimum energy take level was high, some EWHs experienced an energy take of approximately 0 until there was hot water usage. This can be observed from 8:00 to 9:00 as the boxes were shifting above.

At 9:30 (Fig. 12, bottom), the upper whisker was lower than that of 9:00 as the EWHs with most energy take were On to maintain user comfort. The 25% percentile and median at 9:30 were higher than those of 9:00, indicating that more EWHs had higher energy take. At 10:00, most EWHs had high energy take and the box moved upward, making the 0 energy take value an outlier. If the shed event had lasted longer, the box would keep moving upward and have the minimum and maximum energy take values as stated in Table III. The shed event in the evening lasted for 2 hours and the forms of boxes behaved similarly to the first 2 hours of the morning shed event (7:00-9:00).

The aggregated energy take rose from approximately 20kWh to 510kWh from 7:00 to 9:00 and then remained at around 500kWh until the shed event ended at 10:00 (Fig. 13). Theoretically, each EWH could have 0 energy take when the shed event starts and have 2250Wh energy take when the shed event ends. Practically, the simulated 353 EWHs were not able to have the aggregated energy take as 794kWh because, at any given time step, there were always some EWHs that did not reach the energy take of 2250Wh and others that had more than 2250kWh which were turned On. In this study, the average energy take an EWH can contribute was 1,388Wh maximum.

For the case without DR control, the outliers with low temperature appeared from 7:00 to 9:00 due to high hot water flow (Fig. 14, top). The water temperature increased significantly

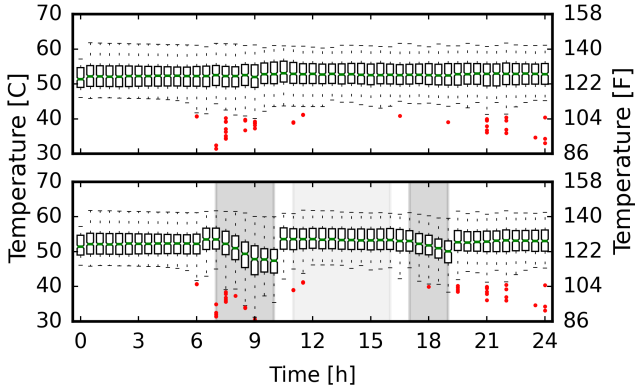

Figure 14. NEW FIGURE–Water temperature in the tank for the EWHs without control (top) and with CTA-2045 control (bottom). The temperature was reduced during the shed event and was maintained high during the load up event in the afternoon.

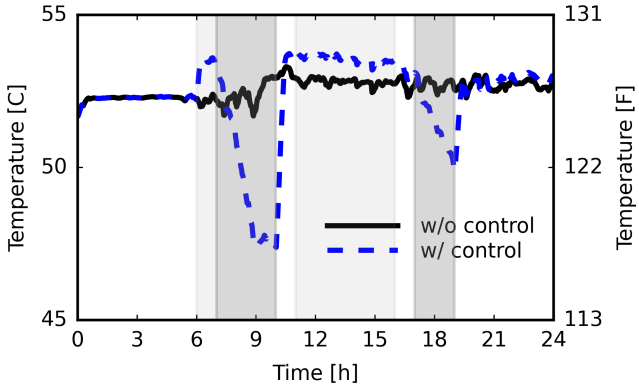

Figure 15. NEW FIGURE–Average tank temperature for all simulated EWHs.

during the first load up event at 6:00. Them temperature at 11:00 did not increase significantly when the load up event started, due to the recovering after the previous shed event. The water temperatures for all EWHs were increased by the load up event in the afternoon, which can be observed clearly from the results at the aggregated level (Fig. 15).

In this study, user comfort was considered violated when the energy take value was more than 2,300Wh. For the case without DR response, 96 EWH had the violation for at least 1 minute, and, with DR control, the number was 171 (Fig. 16). Further insight revealed that most EWHs had short periods of violation for the without control case, e.g., 72 EWHs violated for less than 15 minutes. With the DR control, 51 EWHs had violation minutes of less than 5. The DR control reduced the violation time for some EWHs because of the preheating process under the load up event starting from 6:00. The DR control also caused more EWHs to have more violation minutes due to the shed event. The total violation minutes for all the EWHs was calculated by adding up the violation minutes for each EWH. In total, the case without control had 1,500 violation minutes, and the case with control had 4,033.

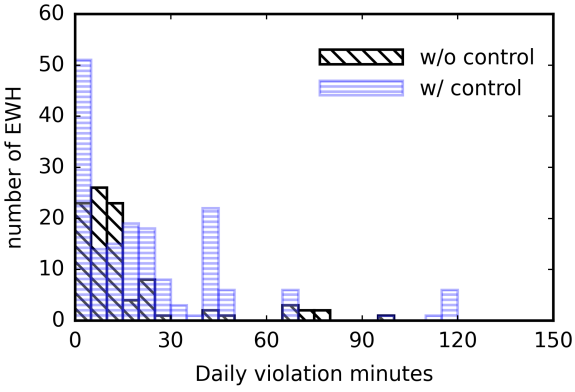

Figure 16. NEW FIGURE–Summary of daily violation minutes for each EWH. Three EWHs had daily violation minutes with [40,50) without control, and this number was 18 with control. With DR control, the number of EWHs with more daily violation minutes increased.

Given a total number of 353, each EWH experienced around 7 minutes more of comfort violation.

VI. Case Study for the Power System

The modified IEEE 123-bus feeder system was used for the simulation with its loads replaced by the sum of EWH power and residential load of each house (Fig. 17). Each residence was assumed to have a 10kW maximum and the default kW value of each node was referred by [15] as "spot loads". A total of 353 different residential profiles were selected from the SET project [17]. Residences were attributed to each of the nodes in the IEEE 123-bus feeder. The system was populated with the representative residences by assigning a randomly selected residence from among the 353 total to an available connection point, or node, which had belonged to pre-existing spot loads from the original IEEE 123-bus example system.

The total power demand for the simulated IEEE 123-bus (Fig. 18) were acquired with the OpenDSS command `circuit.TotalPower`, and only the active power (kW) is presented. Peaks were observed at 6:00 when the load up event occurred and at 10:00 and 19:00 when the shed event ended, as has been explained in the previous section (Fig. 11). The peak power from 7:00–10:00 was reduced from 983kW to 706kW, a reduction of 28%.

The combined use of OpenDSS commands of `circuit.AllBusNames`, `circuit.SetActiveBus`, and `circuit.ActiveBus.puVmagAngle` returned 278 voltage values. If a bus has three phases, the voltages of Φ-1, Φ-2, and Φ-3 were recorded separately. All the voltage (Fig. 19) were within the tolerance of 1±0.05 p.u., although large variations were observed at 6:00, 10:00, and 19:00.

For most of the cases, many of the bus voltages were higher than 1 p.u., as the simulated total residential loads were smaller than the spot loads in the original IEEE 123-bus cases. For example, node 2 had an original spot load of 20kW but was replaced by 2 residences, which could not reach such high

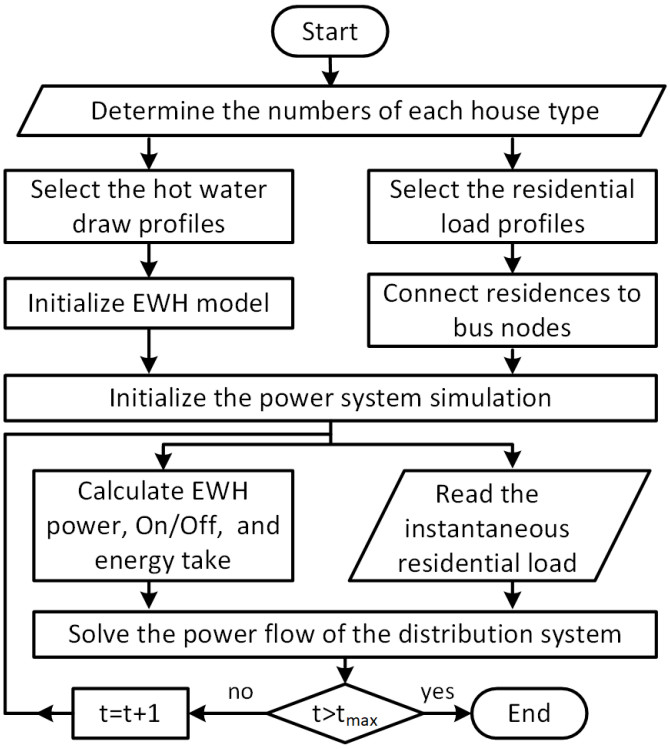

Figure 17. NEW FIGURE–Work flow for the simulation of the distribution power system with realistic residential load and water heater power.

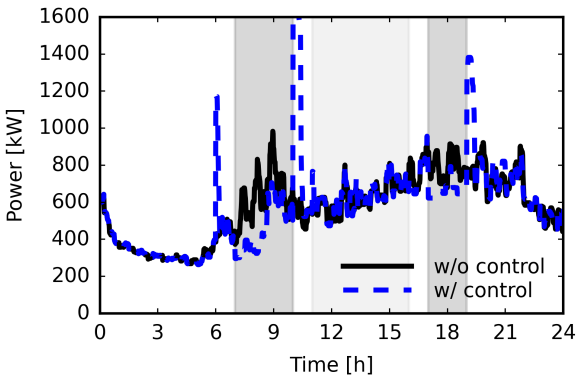

Figure 18. NEW FIGURE–The aggregated residential load for all houses. The shed command postponed the peak power in the morning and evening for this distribution system.

power demand. Therefore, the voltage for the entire simulated power system was more than 1 p.u. for most of the time.

Bus voltages for selected hours were presented in Fig. 20 to show the impact of DR controls. The samples with the same marks for both cases were taken from Fig. 20. When the load up event occurred at 6:00, the voltage for most buses dropped as power demand at most buses went high.

The shed event occurred at 7:00, and the bus voltage went higher as power demand reduced. At 9:00, the 75% percentile values were lower, indicating the rebound for some EWHs, which were also observed in Figs. 10 and 11. The rebound

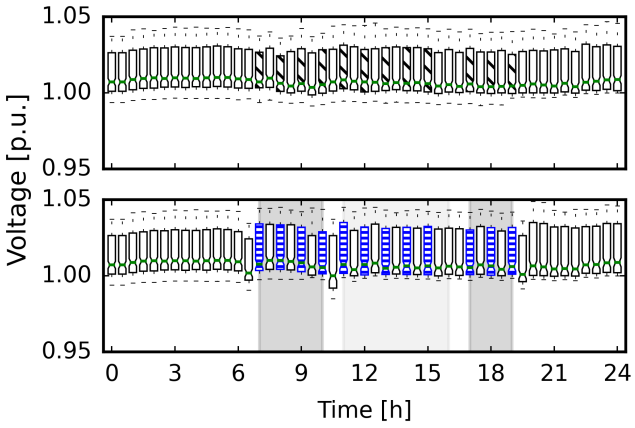

Figure 19. NEW FIGURE–The bus voltages of the IEEE 123-bus system. The boxes during the DR period are marked and compared side-to-side.

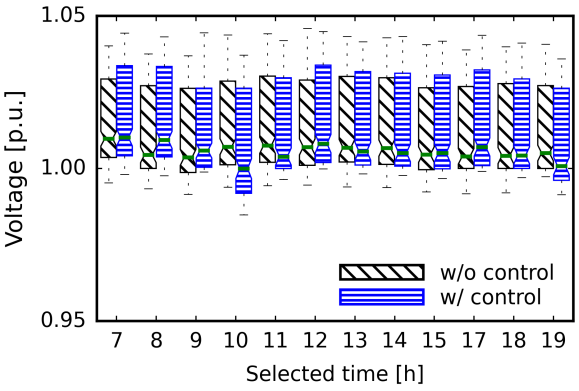

Figure 20. NEW FIGURE–The side-to-side comparison of bus voltages with and without DR control. All the bus voltages were kept within the 5% tolerance during the DR events.

effect was strong at 10:00 when the shed event ended and large power demand from EWHs brought the voltage down.

During the load up event starting at 11:00, most of the buses had lower voltages. The lower whisker was higher than the without control case due to the rebound effect at 10:00, which prevented some EWHs to be turned On at 11:00. The rebound effect at 10:00 and load event at 11:00 antedated the water heating process of most EWHs. Therefore, at 12:00, less EWHs were On and the voltages on buses went higher with DR control. A similar cycle was observed at 13:00, 14:00 (antedated operation) and 15:00 (less EWHs were On) during the load up event.

The voltages increased in general during the shed event in the evening from 17:00. Also observed is the rebound effect at 19:00 when the shed event ended. The DR controls shown above caused the violation of the voltages for all buses within the ±0.05p.u. tolerance, even the power demand was almost doubled in this worst scenario (Fig. 18) .

VII. Conclusion

This paper proposes a generalized approach to energy storage that enables all such systems and devices, not only batteries but also electric water heaters (EWHs) and heating, ventilation, and air conditioning (HVAC) systems, to be controlled with the same variables, namely "energy capacity" and "energy take". Such controls, which were implemented through the Electric Power Research Institute (EPRI) Distributed Energy Resources (DER) integration testbed, comply with the specifications of Energy Star and CTA-2045, which can ensure a platform for industrial and utility adoption. It was found that the example BESS and EWH are comparable when considering their energy content as generalized energy storage (GES) with occupant safety from high water temperatures guaranteed through a mixing valve solution.

A distribution system with 353 residences was simulated using the modified IEEE 123-bus feeder with experimental data and realistic hot water flow. Demand response complying to CTA-2045 specifications was implemented to all the EWHs. In this study, the average energy take value was 1,388Wh at maximum and each residence had 7 minutes more time during which user comfort requirements were not maintained. In this study, all the residences in the same subdivision react to the same DR signal at the same time, reducing the peak power during the shed event by 28%, but leading to higher rebounding peak. Even for this extreme scenario, all the bus voltages were kept within 1±0.05 tolerance throughout the power system.

VIII. Acknowledgment

The support of the Department of Energy sponsored project DE-EE0009021 led by the Electric Power Research Institute (EPRI) is gratefully acknowledged. The support received by Mr. Evan S. Jones through a Department of Education GAANN Fellowship is also gratefully acknowledged.

References

[1] H. Jain, B. A. Bhatti, T. Wu, B. Mather, and R. Broadwater, "Integrated transmission-and-distribution system modeling of power systems: State-of-the-art and future research directions," *Energies*, vol. 14, no. 1, p. 12, 2021.

[2] J. Anandan, "EPRI's DER integration testbed and toolkit," Electric Power Research Institute (EPRI), Tech. Rep. 3002016138, 2019.

[3] B. Ealey, "Overview of epri's der simulation tool for emulating smart solar inverters and energy storage systems on communication networks," Electric Power Research Institute (EPRI), Tech. Rep. 3002013622, 2018.

[4] A. Pratt, M. Ruth, D. Krishnamurthy, B. Sparn, M. Lunacek, W. Jones, S. Mittal, H. Wu, and J. Marks, "Hardware-in-the-loop simulation of a distribution system with air conditioners under model predictive control," in *2017 IEEE Power & Energy Society General Meeting*. IEEE, 2017, pp. 1–5.

[5] J. Lian, Y. Tang, J. Fuller, K. Kalsi, and N. Wang, "Behind-the-meter transactive control approach for home energy management system," in *2018 IEEE Power Energy Society General Meeting (PESGM)*, 2018, pp. 1–5.

[6] H. Gong, E. S. Jones, R. Alden, A. G. Frye, D. Colliver, and D. M. Ionel, "Virtual power plant control for large residential communities using hvac systems for energy storage," *IEEE Transactions on Industry Applications*, pp. 1–1, 2021.

[7] H. Gong, V. Rallabandi, D. M. Ionel, D. Colliver, S. Duerr, and C. Ababei, "Dynamic modeling and optimal design for net zero energy houses including hybrid electric and thermal energy storage," *IEEE Transactions on Industry Applications*, 2020.

[8] "Energy star water heaters - test method to validate demand response," https://www.energystar.gov/products/spec/residential_water_heaters_specification_version_3_0_pd, accessed: 2021-12-14.

[9] "CTA standard: Modular communications interface for energy management," Consumer Technology Association (CTA), Tech. Rep., 2020.

[10] C.Thomas, "Performance test results: CTA-2045 water heater," Electric Power Research Institute (EPRI), Tech. Rep. 3002011760, 2017.

[11] "CTA-2045 water heater demonstration report including a business case for CTA-2045 market transformation," Bonneville Power Administration (BPA), Tech. Rep. BPA Technology Innovation Project 336, 2018.

[12] F. Sossan, A. M. Kosek, S. Martinenas, M. Marinelli, and H. Bindner, "Scheduling of domestic water heater power demand for maximizing pv self-consumption using model predictive control," in *IEEE PES ISGT Europe 2013*, 2013, pp. 1–5.

[13] "CBECC-Res Compliance Software Project," http://www.bwilcox.com/BEES/cbecc2019.html, accessed: 2020-08-04.

[14] K. P. Schneider, B. A. Mather, B. C. Pal, C.-W. Ten, G. J. Shirek, H. Zhu, J. C. Fuller, J. L. R. Pereira, L. F. Ochoa, L. R. de Araujo, R. C. Dugan, S. Matthias, S. Paudyal, T. E. McDermott, and W. Kersting, "Analytic considerations and design basis for the ieee distribution test feeders," *IEEE Transactions on Power Systems*, vol. 33, no. 3, pp. 3181–3188, 2018.

[15] "IEEE PES Test Feeder: 123-BUS Feeder," https://cmte.ieee.org/pes-testfeeders/resources/, accessed: 2021-12-14.

[16] K. Marnell, C. Eustis, and R. B. Bass, "Resource study of large-scale electric water heater aggregation," *IEEE Open Access Journal of Power and Energy*, vol. 7, pp. 82–90, 2020.

[17] H. Gong, V. Rallabandi, M. L. McIntyre, E. Hossain, and D. M. Ionel, "Peak reduction and long term load forecasting for large residential communities including smart homes with energy storage," *IEEE Access*, vol. 9, pp. 19 345–19 355, 2021.

[18] H. Gong, E. S. Jones, A. Jakaria, A. Huque, A. Renjit, and D. M. Ionel, "Generalized energy storage model-in-the-loop suitable for energy star and cta-2045 control types," in *2021 IEEE Energy Conversion Congress and Exposition (ECCE)*. IEEE, 2021, pp. 814–818.

[19] N. Tansangwom and W. Pora, "Development of smart water heater complied with mqtt and echonet lite protocols," in *2018 IEEE International Conference on Consumer Electronics - Asia (ICCE-Asia)*, 2018, pp. 206–212.

[20] H. Gong, E. S. Jones, R. E. Alden, A. G. Frye, D. Colliver, and D. M. Ionel, "Demand response of hvacs in large residential communities based on experimental developments," in *2020 IEEE Energy Conversion Congress and Exposition (ECCE)*. IEEE, 2020, pp. 4545–4548.

[21] A. Magerko, A. Huque, T. Hubert, A. Cortes, and R. May, "Enabling behind-the-meter distributed energy resources to provide grid services," in *2019 IEEE 46th Photovoltaic Specialists Conference (PVSC)*. IEEE, 2019, pp. 2064–2071.

[22] "United states census bureau: Numer of housing unites," https://data.census.gov/cedsci/table?q=bedrooms&tid=ACSDT1Y2018.B25041&vintage=2018&hidePreview=true&g=400C100US45640&moe=false&tp=false, accessed: 2021-12-14.

[23] N. Kruis, P. B. Wilcox, J. Lutz, and C. Barnaby, "Development of realistic water draw profiles for california residential water heating energy estimation," in *Proceedings of the 15th IBPSA Conference San Francisco, CA, USA*, 2017.

[24] H. Gong, T. Rooney, O. M. Akeyo, B. T. Branecky, and D. M. Ionel, "Equivalent electric and heat-pump water heater models for aggregated community-level demand response virtual power plant controls," *IEEE Access*, vol. 9, pp. 141 233–141 244, 2021.